Academic Journal of Engineering and Technology Science
ISSN 2616-5767 Vol.3, Issue 4: 81-89, DOI: 10.25236/AJETS.2020.030409

Synthesis of Dense WS_2 Film and Its Photoelectric Properties

Zhiming Lin*

Department of Electronic Engineer, Jinan University, Guangzhou, Guangdong 510632, China
**Corresponding Author: E-mail:1187362312@qq.com*

ABSTRACT. *As one of the representatives of transition metal sulfides, Tungsten disulfide(WS_2) inherits the characteristics of graphene such as high mobility, transparency and flexibility. At the same time, its wide band gap also makes up for the defect of graphene zero band gap, making it have a higher The switching characteristics of the device make it have a broader development prospect in the field of electronic devices. In this work, low-pressure chemical vapor deposition(CVD) was used to prepare a dense few-layer WS_2 film. At the same time, in order to understand the photoelectric performance of the grown WS_2, a photodetector based on WS_2 was fabricated and its photoelectric performance was studied. Here, the response time and dark current recovery time of the photodetector based on CVD WS_2 is very fast (within 200ms). After illumination, dark current of the device is stable near $7.5e^{-11}$A. Upon Vds = 0.1v, the maximum responsivity of the optoelectronic device is 9mA/W, the maximum EQE is 3%, and the maximum On/Off ratio is 750. The photoelectric performance of the photodetector based on WS_2 from high to low in different wavelength is 405nm, 660nm and 520nm. In addition to preparing photodetectors, this method of synthesizing dense WS_2 film could pave the way for designing Large area humidity or gas sensor to study its humidity sensitive and gas sensitive performance.*

KEYWORDS: *WS_2, Synthesis, photodetector, photoelectric properties*

1. Introduction

In the past decade, two-dimensional materials have received great attention. Because of its better optical and electrical properties, two-dimensional(2D) materials have become the best candidate to replace traditional semiconductor materials [1, 2]. Through research, it was found that graphene has good ductility. Its soft and transparent characteristics will make it also promising in the fields of flexible substrates and displays in the future. Furthermore, layered graphene also has ultra-high mobility and good thermal conductivity. These significant advantages make layered graphene have great development prospects in the fields of optics,

ISSN 2616-5767 Vol.3, Issue 4: 81-89, DOI: 10.25236/AJETS.2020.030409

electricity, and biological detection [3-6]. However, the study found that graphene has no band gap. Compared with electronic switching devices made of traditional silicon materials, its switching ratio is relatively small, which limits its application in the field of electronic devices. As a result, people began to look for other 2D materials. At this point, two-dimensional transition metal sulfides (TMDCs) began to attract people's vision. TMDCs fully inherit the excellent characteristics of graphene such as good ductility, soft, transparent characteristics and excellent mobility. More importantly, it has a band gap which can provide lower cut-off current and higher On/Off ratio so that it can fully compensates for the shortcomings of graphene in this respect [7-10]. Compared with MoS_2 and $MoSe_2$, WS_2 has a larger band gap, stronger photoluminescence characteristics, longer life and higher electron mobility [11-15]. These interesting characteristics show that WS_2 has broader application prospects in the fields of optoelectronics [16-18].

Here, we use low-pressure chemical vapor deposition(CVD) to synthesis dense few-layer WS_2 film. In order to realize the photoelectric performance of this CVD grown WS_2, a photodetector based on WS_2 was fabricated and its photoelectric performance was studied upon different wavelength and different light power density.

2. Experimental

2.1 Synthesis

In this paper, we use CVD to prepare dense few-layer WS_2 film. The procedure was as follows:

1. Substrate cleaning. Whether the substrate is clean or not will greatly affect the chemical meteorological deposition film formation. In this experiment, the Si/SiO_2 sheet was first cut into a square sheet with a size of 1*1cm, and then it was soaked with detergent to remove surface stains. And then separately use acetone (removing detergent), ethanol (removing acetone), deionized water (removing ethanol) for 15 minutes, and finally dry in the drying box and wait for use.

2. Weighing of medicines. Sulfur(S) powder and tungsten trioxide(WO_3) powder is the precursor of growing WS_2. Weigh 500mg of S powder in a quartz boat; 50mg of WO_3 powder is placed on the two corundum pieces at the front of the first long corundum boat (both are 10cm in length), and then placed Si/SiO_2 substrate(SiO_2 face up) on the front of the third long corundum boat as shown in Fig. 1.

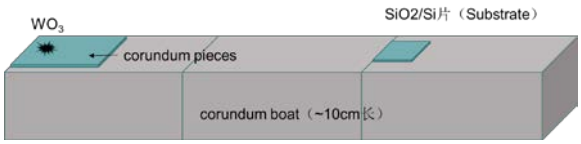

ISSN 2616-5767 Vol.3, Issue 4: 81-89, DOI: 10.25236/AJETS.2020.030409

Figure1. Placement of S and WO_3

3. Clarify the placement of S powder and WO_3 powder in the high-temperature heating furnace SJG-13 (Luoyang Shenjia Kiln Industry Co., Ltd.). The placement of S powder and WO_3 powder has a profound influence on the growth of WS_2. Place the WO_3 powder in the center of the tube-type high-temperature heating furnace, which is convenient for controlling the heating temperature of WO_3 and the growth temperature of WS_2. On the other hand, place the quartz boat filled with S powder at the air inlet of the tube furnace, 6.8cm away from the edge of high-temperature heating furnace as shown in Fig. 2.

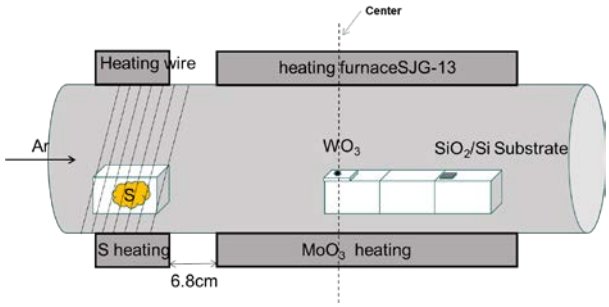

Figure 2. CVD system model diagram of WS_2

4. Reaction conditions. After sealing the tube furnace in which the precursor (S, WO_3) and the substrate are placed, the internal pressure of the tube is pumped to the lowest ($1E^{-1}$Pa, 20min) with a vacuum pump. Subsequently, 300sccm of argon(Ar) gas was introduced for 15 minutes. During this process, the vacuum pump was still fully evacuated to evacuate the air and water vapor in the heating furnace. After that, gradually close the valve of the vacuum pump to control the pressure drop inside the tube furnace and set its pressure to $2.6E^{2}$Pa. At this time, the heating program of the heating furnace can be started: heating at a constant speed of 73 minutes from room temperature to 1100℃ and then maintaining a reaction time of 1 hour. When the heating temperature reaches 51 minutes, the heating wire of the sulfur powder is immediately energized to increase its temperature to 170 ℃. The detailed experimental process is shown in Fig. 3.

ISSN 2616-5767 Vol.3, Issue 4: 81-89, DOI: 10.25236/AJETS.2020.030409

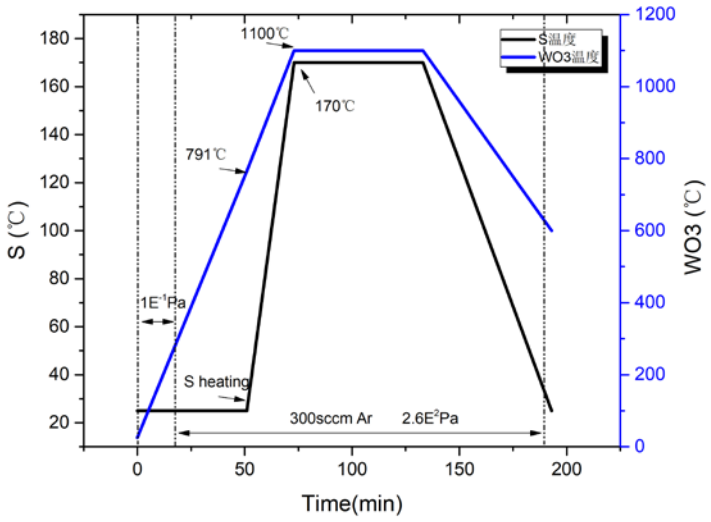

Figure3. Experimental heating curve of synthesizing WS_2

3. Results and discussion

3.1 Characterization of CVD WS_2

In order to analyze the morphology and phase of WS_2 grown by CVD, this paper characterizes WS_2 through three aspects: optical microscope, Raman spectrometer and atomic force microscope.

As shown in Fig. 4, the optical microscope of WS_2 grown under the conditions mentioned above. In Fig. 4a WS_2 grown by CVD is very dense, and some areas of WS_2 have been connected together. Fig. 4b has shown the sparse part of the base WS_2 film. It can be seen that the color of the grown WS_2 is different, which represents the different morphology of the WS_2 film in Fig. 4b. In comparison, the hexagonal WS_2 film on the center of Fig. 4b has a relatively uniform color and a regular shape. Surface of this film is very uniform. In the bottom part of Fig. 4b, films of WS_2 has uneven surface color and very irregular shape, indicating that there is a very obvious dislocation behavior during the growth process. In this article, choose a uniform WS_2 to prepare photodetectors.

ISSN 2616-5767 Vol.3, Issue 4: 81-89, DOI: 10.25236/AJETS.2020.030409

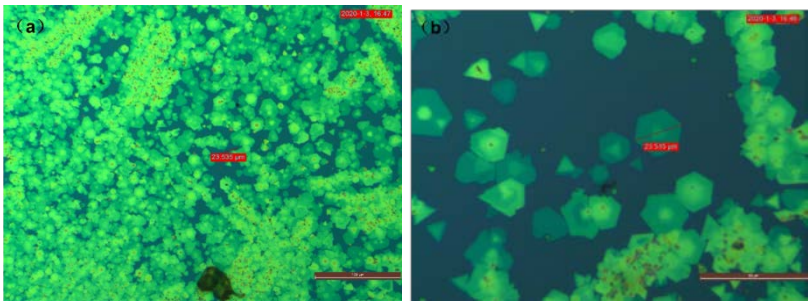

Figure 4. Optical microscope of dense CVD WS_2

As showing in Fig. 5, the triangular WS_2 in the center of the left picture of Fig. 5 is the target WS_2 film irradiated by the micro Raman laser with 514nm, and the right picture of Fig. 5 is the Raman result. According to reports, the Raman characteristic peaks of WS_2 are located in the vicinity of 351cm^{-1} and 416cm^{-1}, respectively[19]. Depending on the number of layers, the distance between the two Raman vibration characteristic peaks under the 514nm laser will vary within the range of 66.8cm^{-1} ~ 71.1cm^{-1}[19]. In Fig. 5, Raman peak difference of the triangular WS_2 central region is 65cm^{-1} which represented the film is a few-layer WS_2.

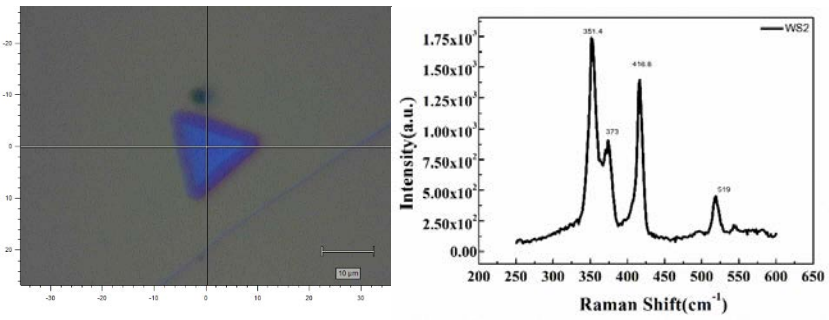

Figure 5. Raman spectra of WS_2. left: Laser irradiation position. right: Raman spectra.

3.2 Photoelectric properties of CVD WS_2 photodetector

Fig. 6a-c show the photocurrent of the photodetector based on WS_2 upon different laser power of 405nm, 520nm and 660nm laser wavelengths, respectively. Illumination takes 20s as a cycle, with light time of 10s and no light time of 10s. In the figure, it can be seen that the photocurrent increase with the increasing light power. This stems from the fact that increasing light power leads to more photons incident on the WS_2 film. The WS_2 film and then absorb more photons and generate more electrons. In addition, photocurrent response time of the WS_2

ISSN 2616-5767 Vol.3, Issue 4: 81-89, DOI: 10.25236/AJETS.2020.030409

photodetector at these three wavelengths is very fast(within 200ms). Photocurrent of WS_2 can be stable to a certain level within 1s of illumination. When the light passes, the dark current recovery time of WS_2 is very fast too. Here, the photocurrent recovers to the original dark current within 200s, and the dark current fluctuates around 7.5e^{-12}A.

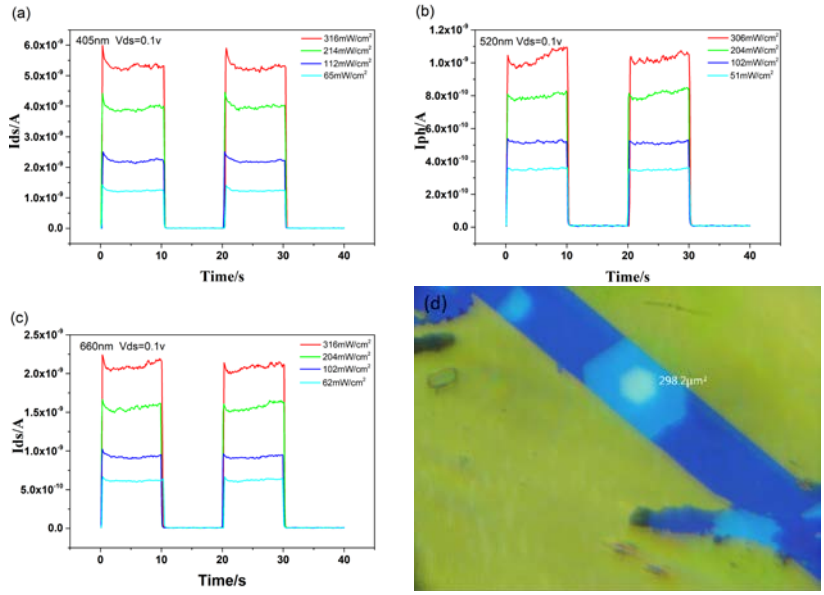

Figure 6. Source-Drain current of Devices. (a)405nm, (b)520nm and (c)660nm for WS_2 photodetector. (d) Micrograph of WS_2 photodetector. V_{ds}=0.1v.

As shown in fig. 7, in order to analyze the specific photoelectric performance of WS_2, this work calculates the photoelectric performance in three aspects(such as responsivity, external quantum efficiency(EQE) and On/Off ratio, respectively based on the data in Figure 6.

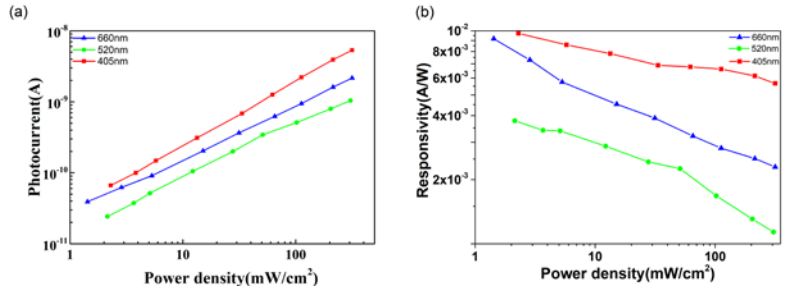

ISSN 2616-5767 Vol.3, Issue 4: 81-89, DOI: 10.25236/AJETS.2020.030409

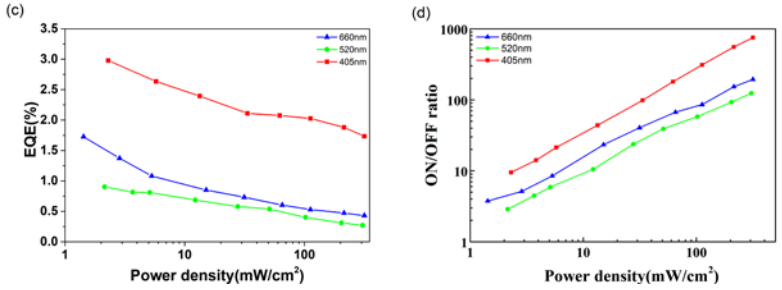

Figure 7. Photoelectric properties of devices. (a) Power density dependent photocurrent and the corresponding (b) responsivity, (c) EQE, and (d) On/Off ratio upon 405, 520, and 660nm illumination. Source–drain voltage: 0.1V.

Fig. 7 presents photoelectric properties based on photodetector of CVD WS_2. Fig. 7a show that the photocurrent increases linearly with the increasing light power density. The photocurrent of the WS_2 photodetector at 405nm wavelength is the largest which is up to the order of e^{-9}A. Although the photocurrent at 520nm and 660nm is relatively lower but it is not much different from the photocurrent at 405nm. Figure 7b shows the responsivity of the WS_2 photodetector under 405nm, 520nm and 660nm wavelength, respectively. The responsivity reaches the highest value of 9mA/W with a light power density of 2.29mW/cm^2 upon 405nm wavelength. No matter which wavelength the optical power density changes, the responsivity is always in the order of 100mA/W. Correspondingly, the external quantum efficiency shown in Figure 7c is similar to the trend of the responsivity graph. However, the external quantum efficiency of the WS_2 photodetector device under 405nm illumination is relatively large, almost three times higher than that under 520nm and 660nm illumination. In Fig. 7d, as the light power density increases, the On/Off ratio curves corresponding to 405nm, 520nm and 660nm wavelength all show a smooth upward trend. This tendency indicates that the dark current stability of the WS_2 photodetector is very good regardless of the wavelength of light (the dark current is stable near 7.5e^{-11}A).

4. Conclusion

In summary, we successfully used CVD to grow dense WS_2 thin film. In order to study the photoelectric performance of WS_2 under this growth condition, WS_2 grown by CVD was prepared as photodetector, and its photoelectric performance was studied. In this paper, the response speed of the photodetector based on WS_2 is very fast (within 200ms). After illumination, the dark current can also be restored to the original dark current within 200ms, and its dark current is stable near 7.5e^{-11}A. Upon V_{ds} = 0.1v, the maximum responsivity of the optoelectronic device is 9mA/W, the maximum EQE is 3%, and the maximum On/Off ratio is 750. Furthermore, this method of synthesizing dense WS_2 film could also pave the way for designing Large

ISSN 2616-5767 Vol.3, Issue 4: 81-89, DOI: 10.25236/AJETS.2020.030409

area humidity or gas sensor to study its humidity sensitive and gas sensitive performance.

References

[1] D. Ovchinnikov, A. Allain, Y. S. Huang, D. Dumcenco and A. Kis (2014). Electrical Transport Properties of Single-Layer WS2. ACS Nano, vol.8, no.8, p.8174-8181.

[2] L. Yang, K. Majumdar, H. Liu, Y. Du, H. Wu, M. Hatzistergos, P. Y. Hung, R. Tieckelmann, W. Tsai and C. Hobbs (2014). Chloride molecular doping technique on 2D materials: WS2 and MoS2. Nano Letters, vol.14, no.11, p.6275-6280.

[3] A. A. Balandin, S. Ghosh, W. Bao, I. Calizo, D. Teweldebrhan, F. Miao and C. N. Lau (2008). Superior Thermal Conductivity of Single-Layer Graphene. Nano Letters, vol.8, no.3, p.902-907.

[4] F. Bonaccorso, Z. Sun, T. Hasan and A. Ferrari (2010). Graphene photonics and optoelectronics. Nature Photonics, vol.4, no.9, p.611-622.

[5] F. Chen, J. Xia, D. K. Ferry and N. Tao (2009). Dielectric Screening Enhanced Performance in Graphene FET. Nano Letters, vol.9, no.7, p.2571-2574.

[6] Y. Song, Y. Luo, C. Zhu, H. Li, D. Du and Y. J. B. Lin (2016). Recent advances in electrochemical biosensors based on graphene two-dimensional nanomaterials. Biosensors and Bioelectronics
vol.76, p.195-212.

[7] A. L. Elias, N. Perealopez, A. Castrobeltran, A. Berkdemir, R. Lv, S. Feng, A. Long, T. Hayashi, Y. A. Kim and M. Endo (2013). Controlled Synthesis and Transfer of Large-Area WS2 Sheets: From Single Layer to Few Layers. ACS Nano, vol.7, no.6, p.5235-5242.

[8] X. Ling, Y. Lee, Y. Lin, W. Fang, L. Yu, M. S. Dresselhaus and J. Kong (2014). Role of the Seeding Promoter in MoS2 Growth by Chemical Vapor Deposition. Nano Letters, vol.14, no.2, p.464-472.

[9] Y. Zhang, J. Shi, G. Han, M. Li, Q. Ji, D. Ma, Y. Zhang, C. Li, X. Lang and Y. Zhang (2015). Chemical vapor deposition of monolayer WS2 nanosheets on Au foils toward direct application in hydrogen evolution. Nano Research, vol.8, no.9, p.2881-2890.

[10] Y. Zhang, Y. Zhang, Q. Ji, J. Ju, H. Yuan, J. Shi, T. Gao, D. Ma, M. Liu and Y. Chen (2013). Controlled Growth of High-Quality Monolayer WS2 Layers on Sapphire and Imaging Its Grain Boundary. ACS Nano, vol.7, no.10, p.8963-8971.

[11] H. ar, A. zden, B. Yorulmaz, C. Sevik, N. Kosku Perkgoz and F. Ay (2018). A comparative device performance assesment of CVD grown MoS2 and WS2 monolayers. Journal of Materials Science Materials in Electronics, vol.29, p.8785–8792.

[12] J. Huang, J. Pu, C. L. Hsu, M. H. Chiu, Z. Juang, Y. Chang, W. Chang, Y. Iwasa, T. Takenobu and L. Li (2014). Large-Area Synthesis of

ISSN 2616-5767 Vol.3, Issue 4: 81-89, DOI: 10.25236/AJETS.2020.030409

Highly Crystalline WSe2 Monolayers and Device Applications. ACS Nano, vol.8, no.1, p.923-930.

[13] A. Kuc, N. Zibouche and T. Heine (2011). How does quantum confinement influence the electronic structure of transition metal sulfides TmS2. Physics.

[14] Y. Li, A. Chernikov, X. Zhang, A. Rigosi, H. M. Hill, d. Z. Van, Arend M, D. A. Chenet, E. M. Shih, J. Hone and T. F. Heinz In Measurement of the optical dielectric function of monolayer transition-metal dichalcogenides: MoS2 , MoSe2 , WS2 , and WSe2, Aps March Meeting, 2014.

[15] D. S. Schulman, A. J. Arnold and S. Das (2018). Contact engineering for 2D materials and devices. Chemical Society Reviews, vol.47, no.9, p.3037-3058.

[16] Z. Jia, J. Xiang, F. Wen, R. Yang, C. Hao and Z. Liu (2016). Enhanced Photoresponse of SnSe-Nanocrystals-Decorated WS2 Monolayer Phototransistor. ACS Applied Materials & Interfaces

vol.8, no.7, p.4781-4788.

[17] N. Perealopez, A. L. Elias, A. Berkdemir, A. Castrobeltran, H. R. Gutierrez, S. Feng, R. Lv, T. Hayashi, F. Lopezurias and S. Ghosh (2013). Photosensor Device Based on Few-Layered WS2 Films. Advanced Functional Materials, vol.23, no.44, p.5511-5517.

[18] C. Ruppert, A. Chernikov, H. M. Hill, A. F. Rigosi and T. F. Heinz (2017). The Role of Electronic and Phononic Excitation in the Optical Response of Monolayer WS2 after Ultrafast Excitation. Nano Letters, vol.17, no.2, p.644-651.

[19] H. Su, C. Wei, A. Deng, D. Deng, C. Yang and J. Dai (2017). Anomalous enhancement of valley polarization in multilayer WS2 at room temperature. Nanoscale, vol.9, no.16, p.5148-5154.